MEASUREMENT OF IONIC CONDUCTIVITY AND TEMPERATURE IN THE APOLLO 15 PLUME

John L. Heckscher, et al

Air Force Cambridge Research Laboratories
L. G. Hanscom Field, Massachusetts

26 February 1973

AFCRL-TR-73-0124
26 FEBRUARY 1973
PHYSICAL SCIENCES RESEARCH PAPERS, NO. 539

AIR FORCE CAMBRIDGE RESEARCH LABORATORIES
L. G. HANSCOM FIELD, BEDFORD, MASSACHUSETTS

Measurement of Ionic Conductivity and Temperature in the Apollo 15 Plume

JOHN L. HECKSCHER
ROBERT P. PAGLIARULO

This research was supported by the Air Force In-House Laboratory Independent Research Fund

AIR FORCE SYSTEMS COMMAND
United States Air Force

Unclassified

Security Classification

DOCUMENT CONTROL DATA - R&D

(Security classification of title, body of abstract and indexing annotation must be entered when the overall report is classified)

1. ORIGINATING ACTIVITY *(Corporate author)* Air Force Cambridge Research Laboratories (LIE) L. G. Hanscom Field Bedford, Massachusetts 01730	2a. REPORT SECURITY CLASSIFICATION Unclassified 2b. GROUP

3. REPORT TITLE

MEASUREMENT OF IONIC CONDUCTIVITY AND TEMPERATURE IN THE APOLLO 15 PLUME

4. DESCRIPTIVE NOTES *(Type of report and inclusive dates)*

Scientific. Interim.

5. AUTHOR(S) *(First name, middle initial, last name)*

John L. Heckscher
Robert P. Pagliarulo

6. REPORT DATE 26 February 1973		7a. TOTAL NO. OF PAGES 27 28	7b. NO. OF REFS 14
8a. CONTRACT OR GRANT NO.	ILIR	9a. ORIGINATOR'S REPORT NUMBER(S) AFCRL-TR-73-0124	
b. PROJECT, TASK, WORK UNIT NOS 46031701	Task 6-70 ILIR-00-01		
c. DOD ELEMENT 62101F	61101F	9b. OTHER REPORT NO(S) *(Any other numbers that may be assigned this report)* PSRP No. 539	
d. DOD SUBELEMENT 681000			

10. DISTRIBUTION STATEMENT

Approved for public release; distribution unlimited.

11. SUPPLEMENTARY NOTES This research was supported by the AFCRL Laboratory Director's Fund	12. SPONSORING MILITARY ACTIVITY Air Force Cambridge Research Laboratories (LIE) L. G. Hanscom Field Bedford, Massachusetts 01730

13. ABSTRACT

Positive ion conductivity and temperature of plume gases enveloping the top of the launcher umbilical tower (LUT) were monitored during the launch of Apollo 15. The measurements are presented along with the orientation of the rocket plume relative to the instrumentation. Details and limitations of the apparatus are described, and the calibration techniques are given.

DD FORM 1 NOV 68 1473

Unclassified

Security Classification

14. KEY WORDS	LINK A		LINK B		LINK C	
	ROLE	WT	ROLE	WT	ROLE	WT
Rocket exhaust						
Conductivity						
Plume conductivity						
Apollo 15						
Ionic conductivity						
Plume temperature						

AFCRL-TR-73-0124
26 FEBRUARY 1973
PHYSICAL SCIENCES RESEARCH PAPERS, NO. 539

IONOSPHERIC PHYSICS LABORATORY PROJECT ILIR
AIR FORCE CAMBRIDGE RESEARCH LABORATORIES
L. G. HANSCOM FIELD, BEDFORD, MASSACHUSETTS

Measurement of Ionic Conductivity and Temperature in the Apollo 15 Plume

JOHN L. HECKSCHER
ROBERT P. PAGLIARULO

This research was supported by the Air Force In-House Laboratory Independent Research Fund

AIR FORCE SYSTEMS COMMAND
United States Air Force

Abstract

Positive ion conductivity and temperature of plume gases enveloping the top of the launcher umbilical tower were monitored during the launch of Apollo 15. The measurements are presented along with the orientation of the rocket plume relative to the instrumentation. Details and limitations of the apparatus are described, and the calibration techniques are given.

Contents

Illustrations

Illustrations

Tables

Measurement of Ionic Conductivity and Temperature in the Apollo 15 Plume

I. INTRODUCTION

Newman et al (1967) demonstrated that lightning could be induced to strike small rockets towing the free ends of grounded wires toward thunderclouds. From these experiments the concept evolved that if a rocket exhaust were sufficiently conducting over a long enough distance, it might behave somewhat as a wire and trigger a stroke. The credibility of this idea was considerably enhanced when Apollo 12 was struck during its first stage burning (NASA, 1970). To investigate this potential hazard to aerospace vehicles and to try to devise a countermeasure capability, the AFCRL Laboratory Director's Fund Project 6-70—"Lightning Strokes to In-Flight Missiles"—was initiated in FY70.

Given certain atmospheric conditions, one way to define the lightning threat is by the percent of actual launches which trigger discharges. A great many events would be required to insure statistical reliability, however, thus making such an approach uneconomical. Taking a lead from the successful experiments by Newman, we can try to simulate a large rocket with its conducting plume by using a small rocket towing a wire of appropriate physical and electrical characteristics. Different rockets will require different wires, since exhaust plume composition depends on such parameters as fuel, size, and trajectory. In the flames of most rocket exhausts, ion concentrations are sufficiently high to insure good electrical

(Received for publication 20 February 1973)

conductivity (Lawton and Weinberg, 1969, p. 214). In the burnt gas regions outside the visible exhaust, however, recombination causes the ion density to fall. Alternating current (AC) methods for measuring conductivity—by propagating microwaves through the plume or by making the plume part of a resonant circuit—are insensitive to the ion concentrations thought to be present in the burnt gas regions (Lawton and Weinberg, 1969 p. 178ff). Nevertheless, these regions may be of sufficient size and conductivity to transfer appreciable charge when exposed to the strong electric fields found near thunderclouds.

Direct current (DC) techniques have long been employed by atmospheric physicists to measure the very small ionic conductivity of the air. In the usual method, an axial flow of air between two coaxial, cylindrical electrodes is subjected to a radial electric field, and the ions attracted toward the center electrode cause a current in the external circuit. This current is a function of the air conductivity, as long as the flow is sufficient to prevent all the ions from being collected. We adapted this technique for use in measuring the positive ion conductivity of rocket plumes, by using all solid-state electronics and by employing construction rugged enough to withstand the launch pad environment.

Through the cooperation of SAC, SAMSO, and SAMTEC, experiments were conducted at Minuteman and Atlas launch sites on Vandenberg AFB, California during FY71 (Heckscher, 1972). Part of the original apparatus was redesigned to fit interface requirements at Kennedy Space Center, and was mounted near the top of the Apollo 15 launcher umbilical tower (LUT) on level 340. Five sec after lift-off, the equipment was activated and the surrounding gases were sampled for about 2 min.

2. EXPERIMENTAL RESULTS

Figure 1 shows the conductivity and temperature recorded during launch, using a linear time scale. To illustrate the geometric relationship between the Saturn exhaust port, the exhaust plume axis, and the instrumentation on the LUT, (1) the altitude of the exhaust port above the horizontal plane containing the instrumentation is superposed on the linear time scale in Figure 1, and (2) the horizontal distances between the LUT, the plume axis, and the exhaust port are shown for various times in Figure 2.

Both conductivity and temperature variations began at about T + 15.25 sec, when the instrumentation was 160 m below the exhaust port and displaced about 32 m from the exhaust axis. Long and short range photographs, taken at the moment of signal onset, are shown in Figures 3 and 4. Rapid and erratic conductivity signals last for almost 6 sec, then become relatively steady, and

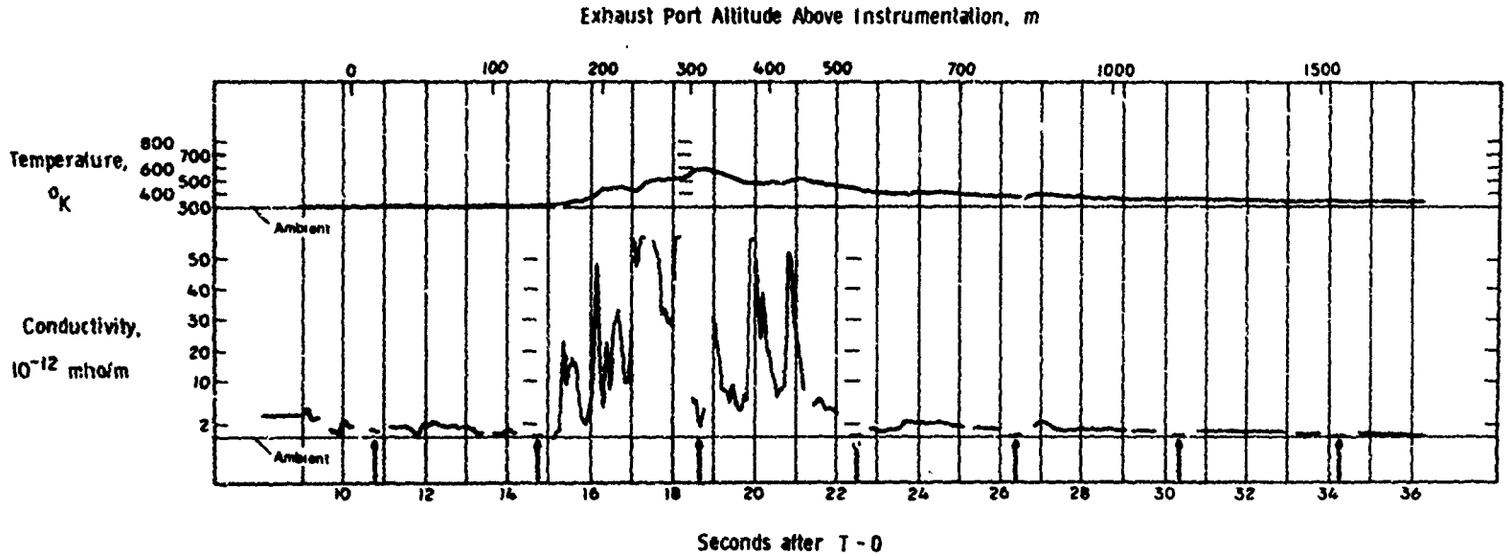

Figure 1. Conductivity and Temperature From T+9 sec Through T+36 sec. Arrows indicate portions of conductivity trace for which chamber voltage was off

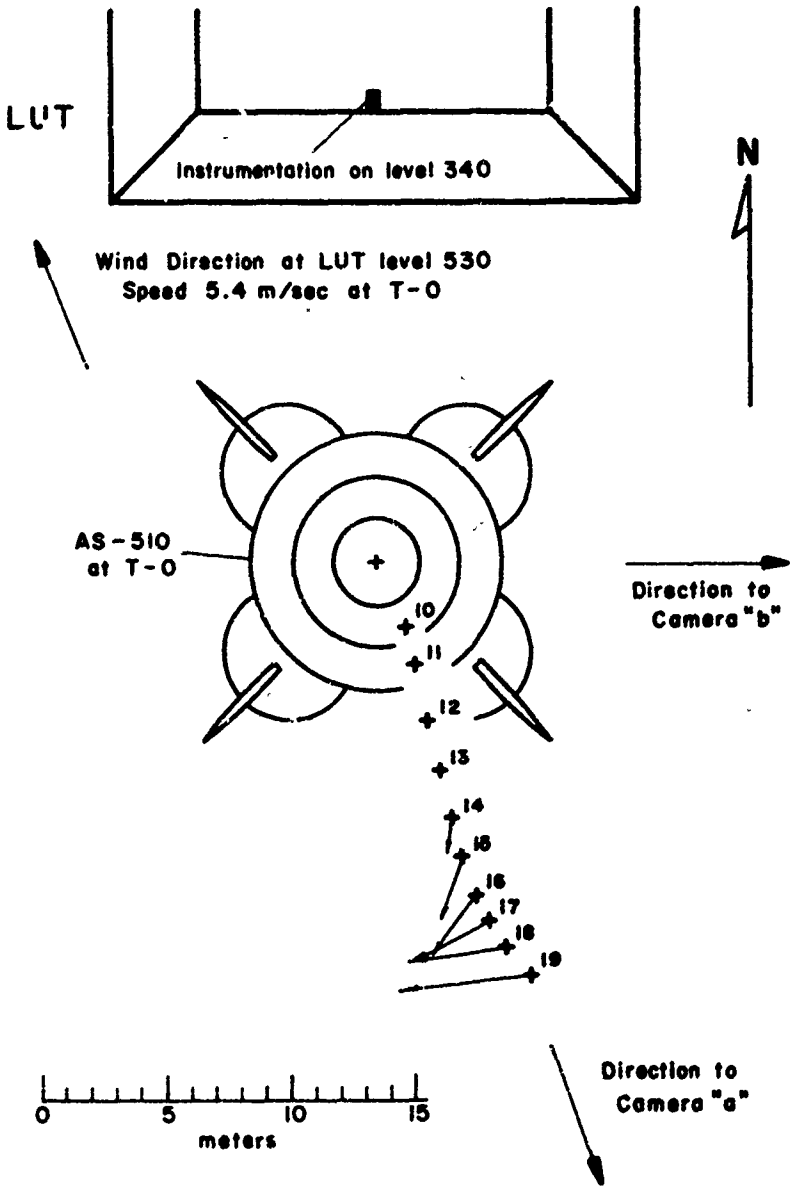

Figure 2. Plan View of the Launch Site, With Relative Positions of the LUT and Apollo 15 (AS-510) at T-0. Crosses show track of center engine gimbal, and the adjacent numbers indicate seconds into launch (NASA, 1971c). Arrows show projection of exhaust axis onto the horizontal plane containing the instrumentation (NASA, 1972). Wind direction and speed obtained from an anemometer atop the LUT are shown (NASA, 1971d), as well as the bearings of the two cameras "a" and "b"

Figure 3. Camera "a" Photograph of Apollo 15 at T+16 sec, Viewed From 160° Azimuth at a Range of About 5.5 miles (NASA, 1971a)

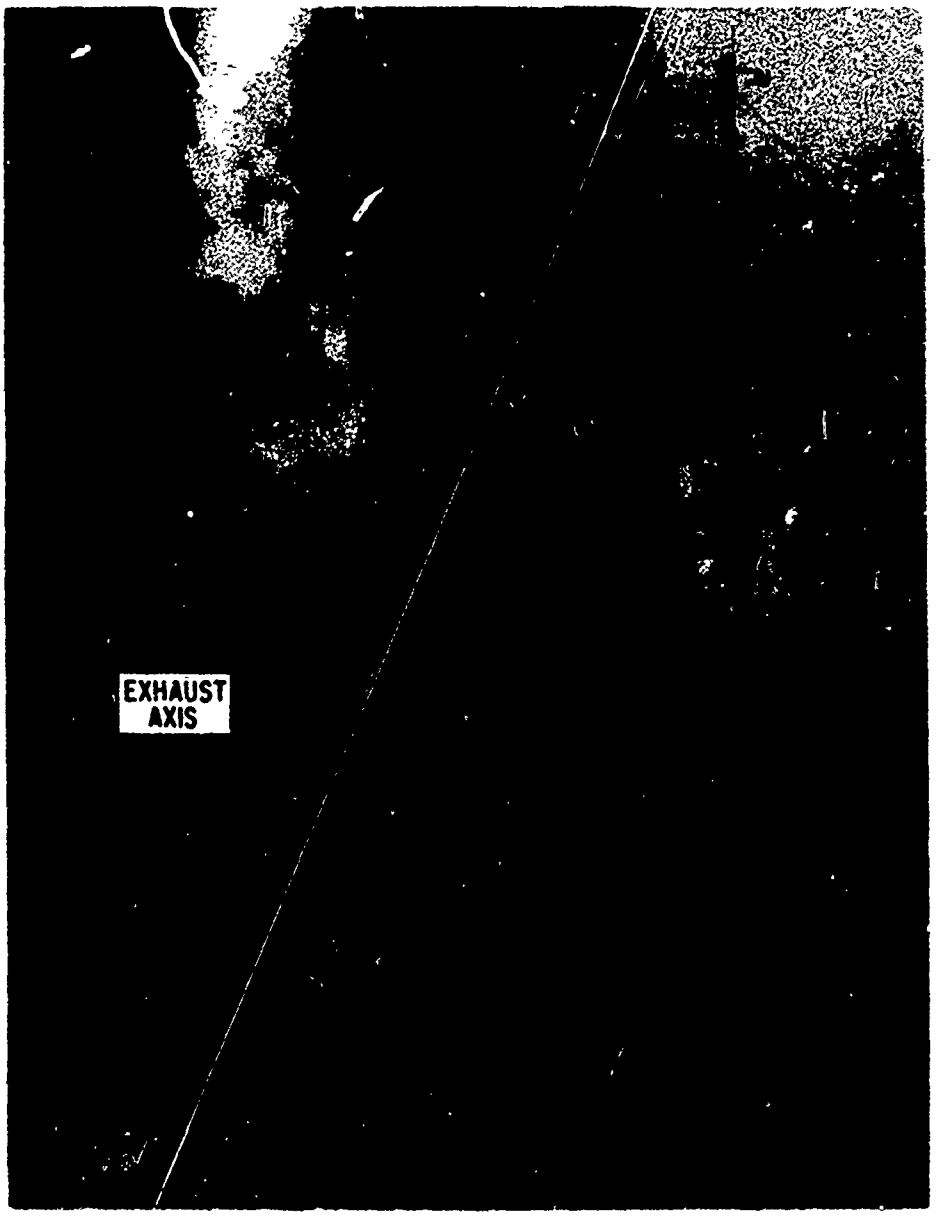

Figure 4. Camera "b" Photograph of Apollo 15 LUT at T+15.25 sec, Viewed From 90° Azimuth at a Range of About 700 ft (NASA, 1971b). The approximate location of the instrumentation is indicated by the arrow

slowly decrease toward the noise level, with occasional small fluctuations. The abrupt change in signal characteristics occurs for an exhaust port altitude of 430 m, with approximately 40-m horizontal distance between the LUT and the plume axis. Conductivity remained higher than 10^{-12} mho/m for exhaust port altitudes up to 1500 m.

In Figure 1, the arrows point to segments of the conductivity trace when the chamber voltage was switched off, to test for the presence of charged particles in the exhaust gases (see Appendix A). Two of these segments, at T + 10.8 and T + 14.7 sec, occur prior to onset of temperature rise and hence prior to envelopment of the equipment by the plume. At T + 18.6 sec, the order of magnitude reduction in conductivity is an indication that charged particle currents are insignificant relative to ionic conduction currents. In subsequent test intervals, the signal reduction indicates a similar situation. The switching process produces transients on the conductivity trace (see Appendix C) which have been omitted for clarity in Figure 1.

3. INTERPRETATION

Evidently, the variations in the two curves of Figure 1 are correlated; that is, a conductivity increase is accompanied by a corresponding rise in temperature. This is consistent with theory showing ion mobility to be inversely proportional to gas density, assuming the ideal gas law to be in effect (Lawton and Weinberg, 1969, p. 115). The erratic behavior may be due partly to the transient voltage response (Figure B2), but is more likely due to the exhaust becoming nonuniform as the high velocity plume mixes with the atmosphere. Since the sample size in the conductivity chamber is small, the rapid changes in conductivity are observed.

There is evidence that the flame did not contact the LUT. The indicated temperature peaked at 600°K, whereas, in the visible plume, temperatures are of the order of 2000°K (Uman, 1970, p. 21). Photographs show no luminosity or clouds nearer than about 20 m to LUT level 340. Finally, the vehicle trajectory and plume orientation were such that the exhaust axis never was pointed directly at the instrumentation (see Figure 2). Surface winds tended to carry the plume toward the LUT; however, the wind speed was very small (5.4 m/sec) compared with the axial exhaust velocity (about 300 m/sec at 360 m behind the exhaust port). At T + 22 sec the gases took about 0.5 sec to travel the 500 m vertical distance from the exhaust port to LUT level 340, so the horizontal displacement due to the wind was only about 3 m.

In Uman's analysis, conductivity is given along the entire plume at a specific time (Uman, 1970, p. 21), whereas our data were obtained as a function of time

at a specific altitude. Strictly speaking, the two are comparable only at T + 35 sec when the Apollo is at 6000 ft. The measured conductivity and temperature are reasonably consistent with the theoretical values of between 10^{-11} and 10^{-13} mho/m, and 400^{o}K.

1. CONCLUSIONS

In the region from 160 m to 430 m behind the exhaust port and between 32 m and 40 m from the plume axis, the conductivity varied erratically; at times it attained values greater than 50×10^{-12} mho/m, with concurrent temperature fluctuations reaching a peak of about 600^{o}K. As the vehicle altitude increased higher than 430 m above the instrumentation, both conductivity and temperature decreased smoothly toward ambient values. Photographs and trajectory data, along with the maximum recorded temperature, provided evidence that the instrumentation was not bathed by the hot gases in the luminous plume, but rather sampled the cooler, burnt gas regions. These data are reasonably consistent with a theoretical Saturn V plume study.

Acknowledgments

We are grateful to Mr. A.J. Carraway, Chairman, KSC Lightning Committee, his associates P. Toft, J. Deese, R. Lupo, R. Wojtasinski, and many others at KSC for making their facilities available and for assisting us in implementing this experiment. In addition, the support provided by Mr. B. Birnhak and other Federal Electric Corporation personnel at KSC is deeply appreciated.

The equipment described in this report evolved from a design by our associate, Mr. R. Harvey, whose keen appreciation of the problems of making measurements in the field contributed in large measure to the success of the experiment. We thank Dr. M. Brook of the New Mexico Institute of Mining and Technology for useful suggestions concerning the precipitation current problem.

We are especially indebted to Dr. E.A. Lewis; his guidance and insight were crucial to the accomplishment of these measurements, and indeed made them possible.

This work was financed through the AFCRL Laboratory Director's Fund, Project 6-70.

References

Burr-Brown (1970), FET and Varactor Operational Amplifiers, PDS-234, Burr-Brown Research Corporation, Tucson, Arizona, p. 2f.

Chalmers, J.A. (1967) Atmospheric Electricity, Pergamon Press, Oxford.

Heckscher, J.L. (1972) Measured electrical parameters and the effective length of rocket exhaust plumes, Proceedings, AFSC 1972 Science & Engineering Symposium, Vol. II, AFSC-TR-72-005.

Lawton, J. and Weinberg, F.J. (1969) Electrical Aspects of Combustion, Clarendon Press, Oxford.

NASA (1970) Analysis of Apollo 12 Lightning Incident, MSC-01540, Manned Spacecraft Center, Houston, Texas.

NASA (1971a) KSC No. 71-60891, IS-DOC-2, Kennedy Space Center, Florida.

NASA (1971b) KSC No. 71-60889, IS-DOC-2, Kennedy Space Center, Florida.

NASA (1971c) Apollo 15 Trajectory, S&E-AERO-YT/G. Daniels, Marshall Space Flight Center, Alabama.

NASA (1971d) AS-510 Launch Wind Data, S&E-AERO-YA-131-71, Marshall Space Flight Center, Alabama.

NASA (1972) Plume Angle Data, S&E-AERO-DFD/G. Ernsberger, Marshall Space Flight Center, Alabama.

Newman, M.M., Stahmann, J.R., Robb, J.D., Lewis, E.A., Martin, S.G. and Zinn, S.V. (1967) Triggered lightning strokes at very close range, J. Geophys. Res. 72(No.8):4761.

Omega, Calibration Tables for Thermocouples, Bulletin No. CT-1, Omega Engineering, Inc., Springdale, Connecticut.

Uman, M.A. (1970) Electrical Breakdown in the Apollo 12/Saturn V First Stage Exhaust, Research Report 70-9C8-HIVOL-R1, Westinghouse Research Laboratories, Pittsburgh, Pennsylvania.

Valley, S.L. (editor) (1965) Handbook of Geophysics and Space Environments, Air Force Cambridge Research Laboratories, Bedford, Massachusetts.

Appendix A

Design Considerations

A1. IONIC CONDUCTIVITY

A unit volume of gas containing n^+ positive ions and n^- negative ions, with mobilities k^+, k^- and charges $\pm e$ has the specific polar conductivies

$$\sigma^+ = en^+k^+$$
$$\sigma^- = en^-k^- \qquad \text{(A1)}$$

and a total conductivity $\sigma = \sigma^+ + \sigma^-$ (see for instance, Chalmers, 1967, p. 195). At sea level, air conductivity can vary from 8×10^{-15} mho/m to 9×10^{-14} mho/m (Valley, 1965, p. 8-19). At 20,000 ft altitude, the conductivity is higher by an order of magnitude.

Uman (1970) has estimated the conductivity of a Saturn V exhaust plume for the exhaust port at 6000 ft altitude; the dependence of σ with altitude is shown in Figure A1. At 4200 ft and below, the ion-controlled conductivity ranges from 10^{-7} to about 10^{-13} mho/m.

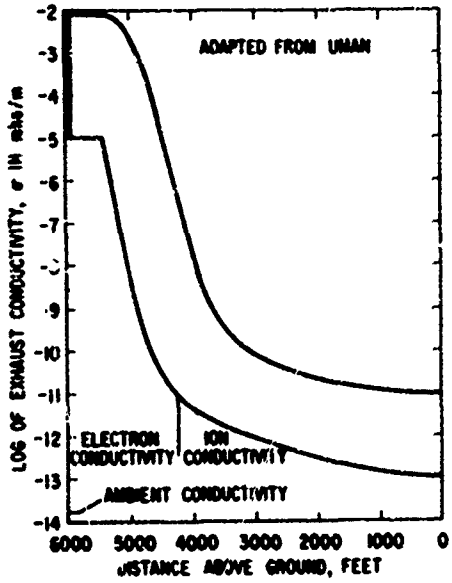

Figure A1. Upper and Lower Limits of Saturn Exhaust Conductivity as a Function of Altitude, for the Exhaust Port at 6000 ft (calculated by Uman, 1970)

A2. POSITIVE ION MOBILITY

Wilson determined the mobility of sodium ions in flame gases to be about 10^{-4} $m^2/V/sec$ (Lawton and Weinberg, 1969, p. 159). Both theory and experiment show that in N_2 at n.t.p., ions of mass greater than N_2 have mobilities between 2×10^{-4} and 3×10^{-4} $m^2/V/sec$ (Lawton and Weinberg, 1969, p. 115). The mobility of small atmospheric ions is between 1×10^{-4} and 2×10^{-4} $m^2/V/sec$ (Valley, 1965, p. 8-3). Evidently, k^+ may be assigned the value 1.4×10^{-4} $m^2/V/sec$, which is often assumed for the mobility of atmospheric ions.

A3. CHAMBER PHYSICAL CHARACTERISTICS

An external view of the instrumentation is shown in Figure A2. One-half in. aluminum stock was used for the housing and baseplate. The conductivity chamber consisted of an outer cylinder, 12-in. long and 2-3/32 in. inside diameter,

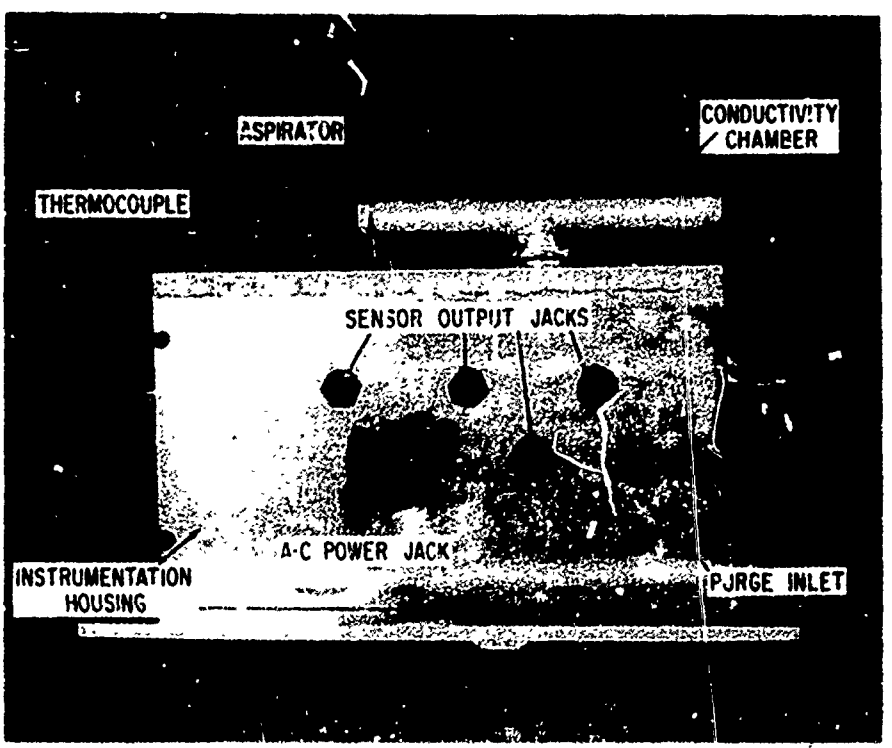

Figure A2. Side View of the Instrumentation Showing the Conductivity Chamber Welded to the Top of the Housing, the Aspirator, the Location of the Gas Temperature Thermocouple, the Purge Inlet, and the Interface Connections

welded to the housing cover, and an inner, coaxial electrode, 10-in. long and 3/8-in. diameter, supported by a perpendicular rod which passed through a teflon insulator into the interior of the housing. An axial flow of gas was maintained by an aspirator with a nominal rating of 24 ft^3/min, mounted on one end of the chamber. The following values (MKS units) were used in the calculations:

a - radius of outer cylinder = 0.0266 m
b - radius of inner cylinder = 0.00476 m
L - length of inner cylinder = 0.254 m
S - cross-section area = 0.00215 m^2
ψ - nominal gas flow = 0.0113 m^3/sec
v - axial gas velocity = 5.26 m/sec

A1. CHAMBER ELECTRICAL CHARACTERISTICS

If the center conductor is at a negative potential V with respect to the outer cylinder, it will attract positive ions, and for a sufficient axial gas flow the current is (Chalmers, 1967, p. 198)

$$i = \frac{\sigma^+ CV}{\epsilon_o} \text{ amp} \qquad \text{(A2)}$$

where C is the chamber capacity, and ϵ_o is the electric permittivity (8.854×10^{-12} farad/m). The capacity C was estimated by comparing calculated and measured values. A 10-in. length of coaxial transmission line with the cross-section of the chamber has a (calculated) capacity of 8.2 pf. This underestimates C, however, since the fringing of the field at the cylinder ends and the capacity of the support rod have been neglected. Several measurements of the capacity averaged 10.3 pf, which overestimates C since the capacity of that portion of the support rod which passes through the insulator—and is not exposed to the ion current—is included. For convenience, C can be taken as 8.854 pf. (that is, numerically equal to ϵ_o in MKS units) with sufficient accuracy for this experiment. Equation (A2) then simplifies to

$$i = V\sigma^+ \text{ amp} \qquad \text{(A3)}$$

and with the chamber operating potential set at 9V by a small carbon-zinc battery, we have

$$i = 9\sigma^{+} \qquad \text{(A4)}$$

relating the measured current to the positive ion conductivity of the gas.

Equation (A4) shows that the chamber current is in the picoampere (pA) range for conductivities of the order of 10^{-12} mho/m. These small currents can be sensed with solid-state "electrometer" operational amplifiers. In Table A1 are shown pertinent characteristics of the Burr-Brown 3336/27 amplifier, designed for use with high impedance current sources. A feedback resistor R_f determines the (output voltage)/(input current) ratio: for R_f less than 10^9 ohm, the input bias current will produce less than 10 μ V at the output with a drift of 1 μ V/^{o}C; hence, resolution is limited by input voltage noise and offset voltage drift. Between 15^{o}C and 35^{o}C, the offset drift should be less than 100 μ V. With R_f fixed at 10^7 ohm, an input current of 9 pA will produce 90 μ V at the output, so the minimum conductivity which can be resolved is about 10^{-12} mho/m. To give rated output the input current is 1 μ A, corresponding to a conductivity of 10^{-7} mho/m.

The conductivity circuit is shown in Figure A3. The negative battery terminal was connected to the inner electrode, and the positive terminal to the amplifier input. Due to feedback this input was at virtual ground, causing the battery voltage to appear across the chamber. With the guard ring also at virtual ground, there was for practical purposes no voltage across the teflon insulator between the guard ring and the outer electrode, and hence no surface conduction current into the amplifier. The 3336/27 amplifier output was conditioned by a linear voltage amplifier to provide a 0 to 5 V output required to interface with LUT recording equipment.

The 3336/27 amplifier output was also applied to a logarithmic voltage amplifier to record the entire range of conductivities. Difficulties, however, with shifting ambient levels made the results questionable, and the data were not utilized (see Appendix C).

A5. ELECTRODE EFFECT

When the electrically neutral, conducting gas enters the chamber, the radial electric field causes the formation of space charge depletion regions around the center electrode and next to the outer cylinder. The electric field will then be perturbed by these space charge regions ("Electrode Effect", see Chalmers, 1967, p. 42f) and the chamber current may no longer be described adequately by Eq. (A4).

Table A1. Specifications for Burr-Brown Model 3336/27 Operational Amplifier (Burr-Brown, 1970)

Input Noise	
Voltage (0.01 Hz to 1.0 Hz)	10 μV p-p
(1.0 Hz to 100 Hz)	5 μV rms
Current (0.01 Hz to 1.0 Hz)	0.001 pA p-p
(1.0 Hz to 100 Hz)	0.002 pA rms
Input Offset Voltage	
at 25°C	adjustable to zero
vs temperature (-25°C to +85°C)	± 10 μV/°C max
vs supply	± 500 μV/V
vs time	± 100 μV/day
Input Bias Current	
at 25°C	± 0.01 pA max
vs temperature (+10°C to +70°C)	0.001 pA/°C
vs supply	0.01 pA/V
Rated Output	
V_o	± 10 V min
I_o	± 5 mA min

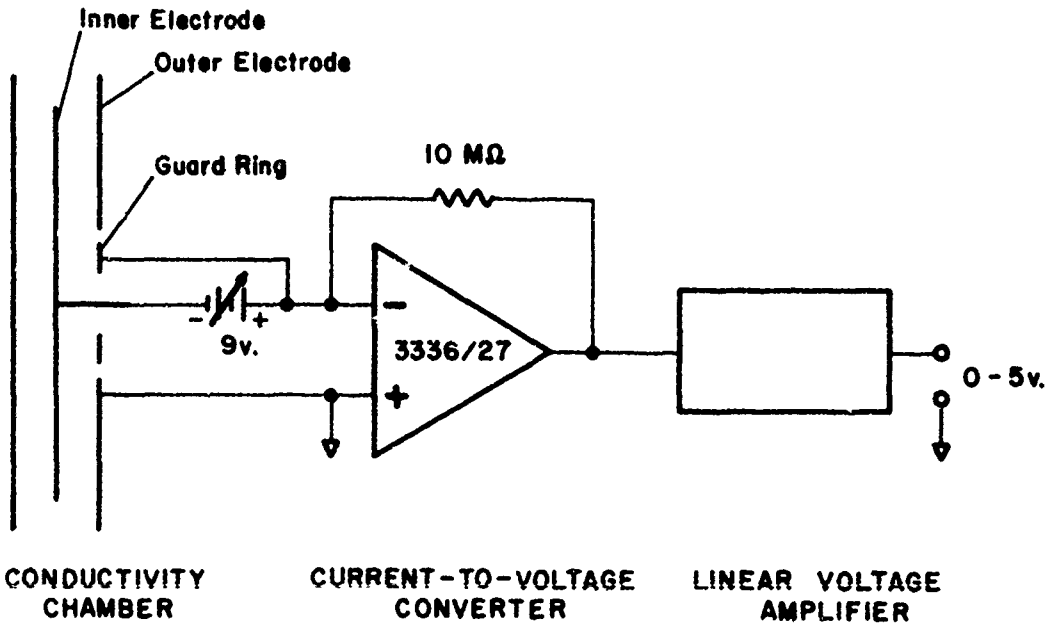

Figure A3. Details of the Conductivity Circuit

Assuming zero axial gas velocity and a uniform charge density in the depletion region, it may be seen that the radial electric field at radius $\underline{r}$ is approximately uniform along the length of the cylinder and given by

$$E(r) \approx \frac{CV - n^+ e\pi L(r^2-b^2)}{2\pi\varepsilon_o rL} \tag{A5}$$

for $\underline{b} \leq \underline{r} \leq \underline{R}$, where $\underline{R}$ denotes the depletion region boundary. This boundary moves radially with velocity $k^- E(R)$, and will reach radius $\underline{P}$ at time τ given by

$$\tau = \int_b^P \frac{dR}{k^- E(R)} . \tag{A6}$$

Performing the indicated integration results in

$$\tau = -\frac{\varepsilon_o}{n^+ ek^-} \log \left[1 - \frac{n^+ e\pi L}{CV}(P^2-b^2)\right] \tag{A7}$$

and solving for the radius $\underline{P}$ we find

$$P^2 = b^2 + \frac{CV}{n^+ e\pi L}\left(1-e^{-\frac{n^+ ek^- \tau}{\varepsilon_o}}\right) . \tag{A8}$$

For a non-zero axial flow of gas, the depletion region will no longer be uniform, but will grow as the gas travels through the chamber. If τ is the time the gas remains in the chamber, we may take Eq. (A8) as giving the maximum radius for the depletion region. Then from Eq. (A5), in order that the radial electric field not be perturbed very much,

$$n^+ e\pi L(P^2-b^2) << CV . \tag{A9}$$

Using Eq. (A8) and rearranging, we find

$$\frac{n^+ ek^- \tau}{\varepsilon_o} << 1 . \tag{A10}$$

Assuming that $k^- \approx k^+$, and since $\tau = L/v$

$$\sigma^+ << \frac{\varepsilon_o v}{L} \quad . \tag{A11}$$

With appropriate values for v and L, we have the requirement that

$$\sigma^+ << 200 \times 10^{-12} \text{ mho/m} \tag{A12}$$

for Eq. (A4) to be valid. Since the maximum conductivity in Figure 1 is about 50×10^{-12} mho/m, no correction for the electrode effect was deemed necessary.

A6. CHAMBER SATURATION

If the gas remains within the chamber long enough to have all the positive ions extracted by the field, the external current becomes a function of the gas flow and ion density, rather than of gas conductivity. This condition, called "saturation", may be avoided by insuring that the axial gas velocity is greater than a minimum given approximately by

$$v_{min} \approx \frac{k^+ CV}{\varepsilon_o S} \text{ m/sec} \tag{A13}$$

for ions of mobility k^+ (see Chalmers, 1967, p. 62f). With appropriate values we find

$$v_{min} \approx 0.5 \text{ m/sec} \, . \tag{A14}$$

The axial velocity maintained by the aspirator, 5.26 m/sec, is more than ten times the minimum required for non-saturated operation.

A7. CHARGED PARTICLE CURRENTS

The incoming gas may contain charged particles more massive than air molecules, some of which will strike the center electrode and give up their charge. If the particles are predominantly of one sign, there will be an effective "precipitation" current whose magnitude might be comparable to, or even exceed the conduction current. Provision was made to periodically test for these currents by

briefly switching off the voltage across the chamber. This should reduce the conduction currents to zero, but have almost no effect on the charged particle currents.

8. TEMPERATURE MEASUREMENTS

The temperature of the gas exiting from the conductivity chamber was monitored by means of a 0.010-in. diameter chromel-constantan wire thermocouple, mounted externally on the housing cover directly under the aspirator (see Figure A2). A second thermocouple inside the housing served as a reference. The temperature of the reference thermocouple was sensed by a thermistor bridge circuit. (See Appendix B for calibration curves.)

Appendix B

Calibration

The relationship between output voltage and gas conductivity was established by connecting very high value resistors across the conductivity chamber electrodes. For example, a 0.1TΩ resistor allows the 9 V battery to supply a current of 90 pA; then by Eq. (A4), this is equivalent to a conductivity of 10×10^{-12} mho/m. Calibration points shown in Figure B1 were obtained when the instrument was set up in the final configuration on the LUT (22 July 1971), during prelaunch calibration (25 July 1971), during post-launch calibration (27 July 1971), and in the laboratory (01 Oct 1971). On launch day (26 July 1971), scheduling and operational requirements limited the calibration to a reading of the ambient level approximately 1 hr after lift-off. The calibration curve was drawn as two straight line segments, from the ambient value at -0.3 V to 10×10^{-12} mho/m at +1.2 V, then to 50×10^{-12} mho/m at +4.8 V.

The response of the output voltage to a step change in current was obtained by connecting and disconnecting a resistor across the chamber, and is illustrated in Figure B2. Note that this does not simulate a step change in the conductivity of the incoming gas, since a finite time is required to completely change the gas in the chamber.

Curves of gas temperature versus output voltage were constructed using standard thermocouple tables (Omega), and are shown in Figure B3. The thermistor bridge calibration curve is given in Figure B4.

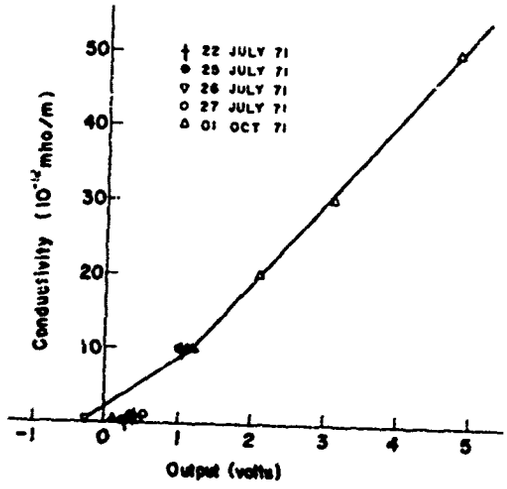

Figure B1. Conductivity Calibration

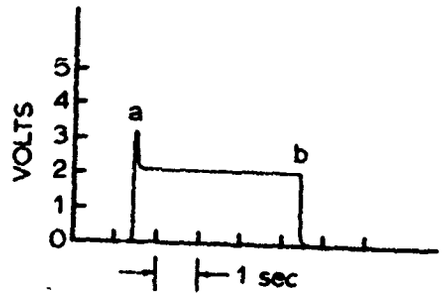

Figure B2. Output of Linear Conductivity Channel When a 50 Gigohm Resistor is Suddenly (a) Connected, and (b) Disconnected Across the Conductivity Chamber Electrodes. The abscissa scale has been made the same as in Figure 1

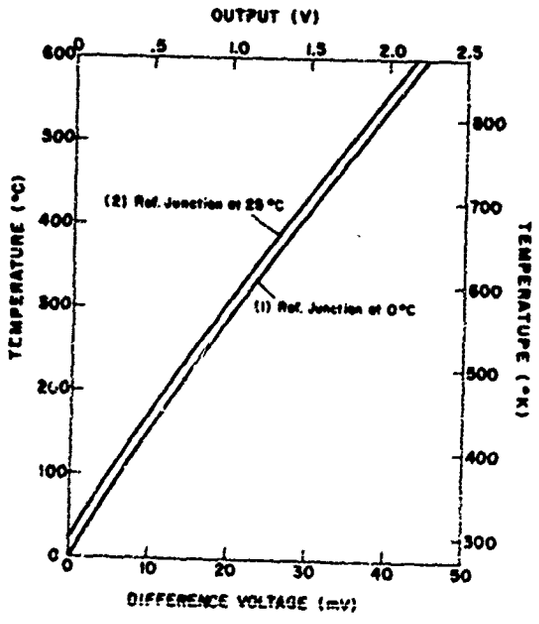

Figure B3. Gas Temperature Calibration

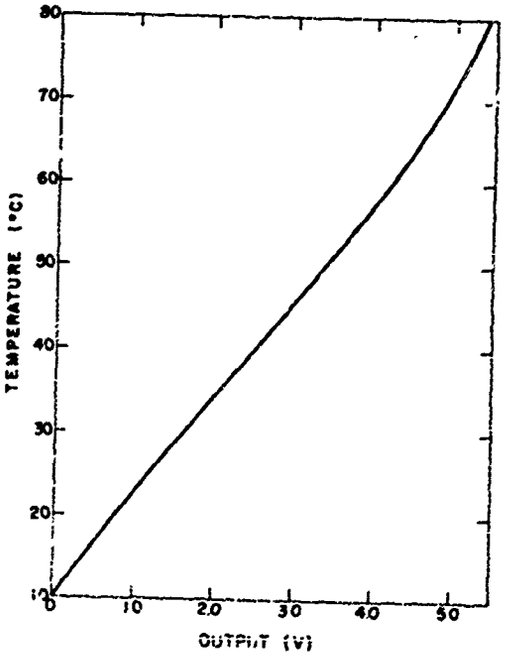

Figure B4. Thermistor Bridge Calibration

Appendix C

Recorded Data

Data were recorded on magnetic tape from T - 30 sec to T + 2 min. The portion between T - 1 and T + 32 sec is shown in Figure C1 as traced from a paper chart playback. Time is indicated by trace e; lift-off, or T - 0, was 207:13:31:00.62.3 Z and is marked by the heavy vertical line. Traces a, b, c, and d show the various output voltage time variations. The horizontal lines a', b', c', and d' are "dummy traces", used to position the calibration levels found both prior to and after data acquisition. Trace f was superposed by hand on the data record; dark portions indicate times when the voltage across the conductivity chamber was switched on (8.2 V—lower bars) and off (0.1 V—upper bars). During the blank intervals the voltage was changing rapidly, causing transients in traces c and d; these are distinguishable by their periodic recurrence, and may be disregarded.

Trace c ("Linear Conductivity") shows a small, high-frequency fluctuation beginning at T + 9.5 sec. A much larger signal starts abruptly at about T + 15.25 sec and continues until T + 21.5 sec. Portions of this large signal are off-scale, and the trace appears clipped. Trace d ("Log Conductivity") shows no large fluctuations. Small deflections occur prior to and during the large variations on trace c. The ambient level of trace d shifts by about 1 V during data acquisition.

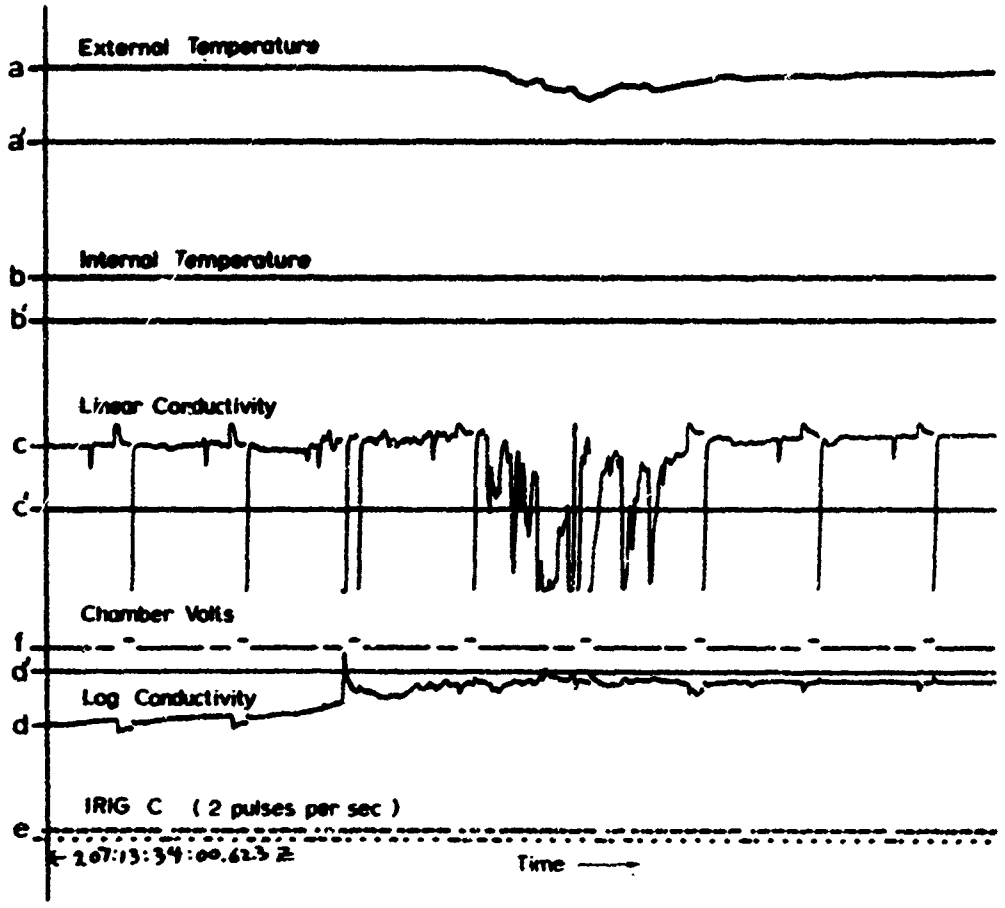

Figure C1. Data Record From T - 1 sec to T + 32 sec. Traces a through e, and a' through d', were recorded during launch. Trace f was drawn by hand to show chamber voltage switching

Trace a ("External Temperature") is constant until T + 15.25 sec, when a break from the baseline occurs. A maximum is reached near T + 18.5 sec. Trace b ("Internal Temperature") is a horizontal line, indicating that the temperature of the internal thermocouple remained constant at about 28°C.